Chemosphere 237 (2019) 124424

Contents lists available at ScienceDirect

Chemosphere

journal homepage: www.elsevier.com/locate/chemosphere

Bioretention cell incorporating Fe-biochar and saturated zones for enhanced stormwater runoff treatment

Jiaqing Xiong [a, b, *], Sihui Ren [b], Yifan He [b], Xiaochang C. Wang [a, b], Xuechen Bai [c], Jiaxuan Wang [d], Mawuli Dzakpasu [a, b, e]

[a] Key Lab of Northwest Water Resource, Environment and Ecology, MOE, Xi'an University of Architecture and Technology, Xi'an, 710055, PR China
[b] School of Environmental and Municipal Engineering, Xi'an University of Architecture and Technology, Yan Ta Road. No.13, Xi'an, 710055, China
[c] China United Northwest Institute for Engineering Design & Research Co., Ltd (CUCED), Zhang Ba Si Road. No.16, Xi'an, 710077, China
[d] School of Architecture and Civil Engineering, Xi'an University of Science and Technology, Yan Ta Road, No. 58, Xi'an, 710054, China
[e] International Science & Technology Cooperation Center for Urban Alternative Water Resources Development, Yan Ta Road. No.13, Xi'an, 710055, China

HIGHLIGHTS

- Iron-coated biochar (ICB) increased the adsorption of the media to phosphorus.
- ICB supplied the carbon source for the denitrification reaction.
- Single-layered experimental columns were more conducive to the removal of nitrate.
- Denitrifying enzyme activity of media is higher at the media boundary.

ARTICLE INFO

Article history:
Received 5 January 2019
Received in revised form
7 July 2019
Accepted 20 July 2019
Available online 22 July 2019

Handling editor: Patryk Oleszczuk

Keywords:
Runoff pollution
Bioretention
Iron-modified biochar
Amended media
Nutrients

ABSTRACT

Nitrogen (N) and phosphorus (P) removal in conventional bioretention systems is highly variable. Therefore, five novel experimental columns with different media configurations and constituents, and incorporating a saturated zone were developed and assessed to optimize the removal of N, P and other nutrients. Three types of media composed of the conventional mixed sand and soil media (T_1), biochar-amended media (T_2), and iron-coated biochar (ICB)-amended media (T_3) were evaluated. Two of the experimental columns were designed with double-layer configurations, while the other three were of a single-layer structure. Removal efficiencies of nutrients in the experimental columns were evaluated and compared using simulated runoff. Also, the effect of media depth on the retention of P and denitrifying enzyme activity (DEA) in the bioretention columns were evaluated. The experimental column only filled with T_3 showed the best performance for COD, ammonia (NH_4^+-N) and total phosphorus (TP) removal (94.6%, 98.3% and 93.70%, respectively), whereas columns filled with T_2 performed poorly for TP removal (57.36%). For the removal of nitrate (NO_3^--N) and total nitrogen (TN), the columns using a single-layer and only filled with either T_3 or T_2 exhibited the best performance (93% and 97% TN removal, respectively). Overall, this study demonstrates that our proposed single-layered bioretention cell only filled with T_3 and incorporating a saturated zone effectively improves the runoff quality, and can provide a new bioretention cell configuration for efficient stormwater treatment.

1. Introduction

Rapid urbanization brings a range of physical and biochemical changes to the urban environment, resulting in considerable increases in stormwater runoff volumes and the degradation of receiving water bodies (Macedo et al., 2019). As a low impact development practice, bioretention systems can simultaneously mitigate the impact of urban stormwater runoff on the hydrology, quality, and ecology of water bodies, which has been widely adopted across the world (Hunt et al., 2012). Although bioretention systems show a high capacity for the removal of some heavy

---

* Corresponding author. Key Lab of Northwest Water Resource, Environment and Ecology, MOE, Xi'an University of Architecture and Technology, Xi'an, 710055, PR China.
E-mail address: xiongjiaqing@xauat.edu.cn (J. Xiong).

https://doi.org/10.1016/j.chemosphere.2019.124424
0045-6535/

metals, suspended solids, oils, and pathogenic bacteria, etc. (Sun and Davis, 2007; Bratieres et al., 2008; Trowsdale and Simcock, 2011; Kim et al., 2012), its performance in the removal of nutrients such as nitrogen (N) and phosphorus (P) is unsatisfactory and varies greatly (Davis et al., 2001, 2009, 2006; Hunt et al., 2006; Hatt et al., 2009; Li and Davis, 2009).

N is closely associated with water quality problems and is an important nutrient that can lead to the eutrophication of a natural water body (Zinger et al., 2013). Stormwater can be an important N source in urban environments and, thus, requires effective treatment (Li and Davis, 2014). N removal by bioretention cells is highly variable and overall ineffective, mainly due to the release of nitrate-nitrogen (NO_3^--N) from the microbial transformation of dissolved organic nitrogen (DON) and ammonium (NH_4^+-N) within bioretention filter media that results in high NO_3^--N effluent concentrations (Li and Davis, 2014; Tian et al., 2019). Nonetheless, studies also show that under suitable conditions, the NO_3^--N retained in the bioretention cell can be transformed to gaseous nitrogen in anaerobic zones through denitrification (Nielsen and Revsbech, 1998). To this end, researchers endeavor to increase the adsorption of NH_4^+-N by making various improvement to the media materials and creating anaerobic conditions by setting a saturated zone to enhance the NO_3^--N removal (Zinger et al., 2013; Tian et al., 2016). However, the effects of the saturated zone on the N removal performance demonstrates a high variability and is influenced by media properties and the presence of electron donor (Hsieh et al., 2007; Lopez-Ponnada et al., 2017). Consequently, no significant improvement to the total nitrogen (TN) removal due to the presence of a saturated zone for nitrate denitrification has been reported (Li and Davis, 2014). Moreover, some researchers (Hsieh et al., 2007; Cho et al., 2009; Wan et al., 2017) have suggested the layering of the media materials to improve NO_3^--N removal. Recent studies demonstrate that wood chips could maintain anaerobic conditions suitable for denitrification to proceed in the upper layer (Wan et al., 2017). Consequently, it is believed that adding biochar only in the upper layer may further enhance these conditions, but no investigation has been reported yet.

Stormwater runoff is also a major source of P in urban environments and requires effective treatment (Liu and Davis, 2014). Total phosphorus (TP) transported by stormwater runoff consists of particulate phosphorus (PP) and dissolved phosphorus (DP) (Davis et al., 2001). Bioretention is highly effective at removing PP but is less successful at addressing DP, because DP removal in bioretention systems mainly depends on chemical P sorption (Davis et al., 2001). Richardson and Vepraskas (2015) pointed out that the removal of P in bioretention systems relies primarily on the absorption of iron oxides into the media materials, and the ability of the media to adsorb P is significantly affected by its iron content. It is suggested that materials rich in iron and aluminum compounds, such as water treatment residuals, may effectively mitigate P leaching from bioretention systems (Liu and Davis, 2014). Therefore, the removal of P may also be improved by incorporating such materials into the media used in bioretention cells. However, this traditional method of amending the media only focuses on enhancing the removal of P, with no consideration for enhancing the removal of N.

In order to simultaneously improve the efficiency and consistency of both N and P removal in bioretention cells, biochar or iron-coated biochar (ICB)-amended single/double-layer systems were designed and tested in this study. Biochar is an organic material with high carbon content, prepared by high-temperature pyrolysis of organic matter under a complete or partially anaerobic environment, which improves its stability (Sun et al., 2018). Aiming at the removal of P, ICB obtained through the modification of biochar by the method of surface activation, was used to amend the media of bioretention systems (Li et al., 2014). This is a new amending technology for bioretention systems, which has been rarely used. Therefore, this article develops a novel ICB-amended media for use in bioretention systems, for the first time. A few studies using laboratory experiments demonstrate the simultaneous removal of N and P by ICB, yet the mechanisms are not elucidated. Furthermore, the use of biochar as a filter material in field-scale bioretention systems has not been investigated.

The incorporation of ICB in the filter media of a bioretention cell is expected to enhance both N and P removal from stormwater runoff in four primary ways. Firstly, biochar amendment may significantly increase soil water retention (Mohanty et al., 2018), which can promote redox conditions conducive for denitrification to proceed. Secondly, biochar amendment could enhance denitrification by acting as an electron donor for denitrifying bacteria (Tian et al., 2019). Thirdly, the high specific surface area of biochar also provides a suitable environment for the growth of attached microorganisms, resulting in significant improvement in the activity of microorganisms (Xu et al., 2014, 2016). Furthermore, it is important for P removal that ICB have a high content of iron, which allows bioretention cell to remove P without external input of iron.

This paper firstly proposes a method for improving the media in bioretention cells by using biochar or ICB and setting saturated zone synchronously. The effects of biochar and ICB on the media are evaluated by comparing the removal of nutrients such as N, P, and the effect of different depths of the media on the retention of TP and denitrifying enzyme activity (DEA) in different experimental columns. Findings from the column experiments are used to optimize the performance of bioretention systems for nutrients removal from stormwater runoff.

2. Materials and methods

2.1. Experimental setup

The experimental columns (Fig. 1) comprise five HDPE cylindrical tanks, each with a diameter of 300 mm and a height of 1250 mm. Each column consisted of four layers from top to bottom: submerged layer (255 mm), mulch layer (100 mm), filter media layer (700 mm) and gravel drainage layer (150 mm). The mulch layer uses gravel with a size of 10–20 mm, and the gravel drainage layer uses gravel with a size of 30–40 mm. The key roles of the mulch layer were to suppress weeds, protect the media surface from water erosion and clogging, and they can be aesthetically attractive and are potentially less likely to clog. The structure and constituents of the filter media layer for each experimental column is different. The media of the control group T_1 was a uniform mixture of 88% C33 concrete sand (SAND) and 12% soil (SOIL) by mass (NCDWQ, 2007). The amended media of experimental group T_2 is composed of a uniform mixture of 96% T_1 and 4% rice husk biochar (RHB). The amended media of experimental group T_3 comprised a uniform mixture of 96% T_1 and 4% ICB. Two experimental columns of double-layer configurations were built by adding biochar in the upper layer of the media to investigate the role of biochar for denitrification. The height of the lower part of the filter media layer is 300 mm, and the upper part is 400 mm. Sampling points were set at different heights along the length of the experimental columns. Upturned water outlets are provided from the bottom of the column for collecting water samples at different submerged heights. The outer walls of the experimental columns were wrapped with a thermal insulation film to reduce the influence of ambient temperature. Furthermore, no plants were planted in the experimental columns to prevent plant interference.

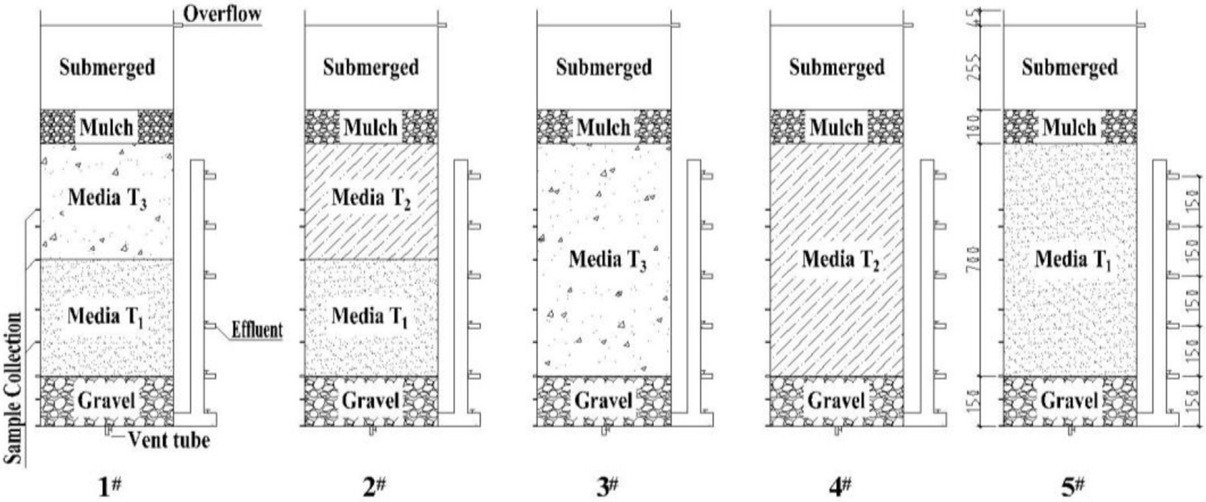

Fig. 1. Number and structure of experimental columns.

2.2. Biochar preparation and modification

RHB is prepared by the thermal cracking method. The pyrolysis heating rate is 15 °C/min, and the highest pyrolysis temperature is 500 °C. The RHB samples were activated with distilled water and 1 mol L^{-1} hydrochloric acid (HCl) solution (Li et al., 2014). The RHB samples (100 g) were soaked in 1 L hydrochloric acid solution for 1 h. The samples were then washed with deionized water until the pH of the washed water was 7.0. Afterward, the samples were dried at 75 °C for 12 h. The above biochar was then mixed with $FeCl_3$($FeCl_3 \cdot H_2O$) solution according to the Iron/carbon mass ratio of 0.70. The pH of the mixed solutions was adjusted to 7.0 with 3 mol L^{-1} KOH. The mixed solutions were left to stand for 1 h and then, washed with distilled water several times and dried at 75 °C. This iron-coated biochar was marked as ICB.

2.3. Characterization of physicochemical properties of media

The pH of the biochar was measured by mixing in a carbon to water ratio (w/v) of 1:20, shaking for 1 h and then leaving the solution to stand for 5 min. The pH of soil and sand were determined by putting 25 g of soil or sand into a beaker and adding 25 mL of deionized water. The mixed liquids were stirred for 15 min. The ash content of the media was determined by weighing about 1 g (accurate to 0.1 mg) of the sample to be tested into a crucible. The open end of the crucible was then placed in a Muffle furnace at 800 °C for 4 h, subsequently cooled to room temperature and taken out for weighing. The ash content was calculated as follows:

$$A = \frac{m_2 - m_1}{m} \times 100\% \tag{1}$$

where A is ash content (%); m is the mass of biochar before burning (g); m_1 is the mass of empty crucible (g); m_2 is the mass of ash and crucible (g).

The test for cation exchange capacity (CEC) used the ammonium acetate method (Tan, 2005a). The exchangeable acidity was determined by potassium chloride extraction-titration (MOEE, 2013). The specific surface area was measured by N_2 adsorption and analyzed with a Brunauer, Emmett, and Teller (BET) isotherm (*_V-Sorb 2800P). The morphology and structure of the samples were analyzed by scanning electron microscopy (SEM) (*_JSM-6510LV) to observe the surface morphology of biochar before and after modification. Fourier transform infrared (FTIR) analysis (Nicolet 6700) of the biochar was performed to identify the surface functional groups. The biochars were analyzed by infrared spectroscopy between 400 and 4000 cm^{-1}, with 50 scans being taken at 2 cm^{-1} resolution. The ζ-potential of the colloidal biochar was determined using a solid surface ZETA potentiometer.

2.4. Equilibrium adsorption by biochar

In practice, after biochar is added to a bioretention system, it is rinsed or leached over time by infiltrating stormwater, which results in weathering and leaching of soluble components. The sorption of ammonia-nitrogen onto leached biochar was examined in batch sorption experiments using RHB and ICB leached with DI water from the leaching experiments. Sorption experiments were performed in duplicate at 20 ± 2 °C (Jing, 2016). A 0.1 mol/L ammonium (NH_4Cl) stock solution was diluted with DI water to achieve initial NH_4^+-N concentrations of 0, 0.5, 1, 2, 5, 7, 10 mg/L. Experiments were carried out in 50 mL glass vials containing 0.1 g of DI-leached biochar and 50 mL of NH_4^+-N solutions with different concentrations in DI (initial pH = ~7.0). Additional vials with NH_4^+-N solutions but no biochar was used as controls. Vials were shaken at 150 rpm for 24 h on a platform shaker, and samples filtered with 0.45 μm syringe filters before measurement. NH_4^+-N concentrations in all filtered solutions were measured. The amount of NH_4^+-N adsorbed onto the biochars was calculated according to the method proposed by Li et al. (2014). Isotherm data were fit to the Langmuir models (Tian et al., 2016). The parameters were deduced from experimental data using non-linear regression. A dimensionless constant separation factor R_L was defined (Tian et al., 2016). The R_L value indicates whether the sorption is favorable ($0 < R_L < 1$), unfavorable ($R_L > 1$), irreversible ($R_L = 0$), or linear ($R_L = 1$).

2.5. Runoff simulation experiment

The effect the saturated zone on the performance of the bioretention basin for rainwater runoff treatment was evaluated by setting the outlet height of the experimental columns at 300 mm. Synthetic runoff was applied to each column at 3.47 mm/h for 6 h using a calibrated Masterflex pump (Halma, London, England). This flow rate was based on a 2.08-cm total rainfall event with a 6-h duration, corresponding to a median annual precipitation event for Xi'an (MOHURD, 2014). With the bioretention area sized at 5% of the drainage area, a rational method synthetical runoff coefficient, c, of 0.8 is assumed to arrive at the design bioretention runoff loading. The runoff coefficient, obtained by a weighted average of plots of different land types, is derived from the specific basin (Xi'an, China), which consist of green lands, squares, residences, and roads. The water distribution uses simulated rainfall to eliminate interference from other conditions. Concentrations of pollutants for use in laboratory stormwater runoff studies were based on runoff sampling data obtained in Xi'an (Jiang et al., 2017). Pollutants concentrations were formulated using glucose at a COD concentration of 300 mg/L, potassium nitrate at NO_3^--N concentration of 8 mg/L, ammonium chloride at NH_4^+-N concentration of 8 mg/L, and monopotassium phosphate at PO_4^--P concentration of 2 mg/L. The test was repeated at intervals of 18 h for 11 consecutive times. Effluent water samples were collected and tested for NO_3^--N, NH_4^+-N, TN, TP, COD and other indicators.

2.6. P retention and denitrification potential of media

Core soil samples were taken along the depth of the column after 11 synthetic runoff applications to investigate P retention and DEA in the bioretention cells. A total of fifteen samples were collected at the depths of 250, 550, and 700 mm from bottom to top. 1 g of each soil sample was placed in a crucible, dried at 105 °C for 24 h to measure the water content. The remaining samples were tested by air drying (Tan, 2005b). Denitrification potential of the media was determined by measuring the DEA (Sun et al., 2018). Moreover, the P interception efficiency at different heights in the media was calculated with the following equation :

$$B = \frac{(m_e - m_0)}{m} \tag{2}$$

where B is the P interception efficiency (mg/g); m_0 and m_e (mg) are the TP contents of the media at the beginning and end of the experiment, respectively; m is the mass of the media (g). TP contents of the media were determined by the alkali fusion-mo-sb anti spectrophotometric method (MOEE, 2014).

3. Results and discussion

3.1. Physicochemical characteristics of media

Table 1 shows the chemical and physical characteristics of the pure media. As expected, the pH of the ICB is the lowest, while those of the RHB and SAND are relatively similar. The pH of the SOIL is neutral. The acidic pH of the ICB may be attributed to the use of hydrochloric acid in the modification process. In addition, ash contents of both ICB or RHB were significantly lower than those of SOIL and SAND. Nonetheless, the ash content of ICB is lower than that of RHB, indicating that ICB has more organic components and can be used in bioretention systems to augment the carbon source for denitrification processes. At the same time, the CEC of the ICB is higher than that of the RHB, which may be due to the loading of ferric ions on the ICB. At the pH of 7, the ζ-potential of all media is negative, and the ζ-potential of the ICB is lower than that of the RHB. ICB and RHB had, by far, the highest surface areas of all the media. The surface area of the RHB was about 13% less than that of the ICB. The sand was calcareous and had a fairly high surface area for sand, which may be due to the presence of silt and clay particles. Overall, the CEC, ζ-potential and specific surface area of the ICB are better than those of RHB, indicating that ICB could have better adsorption performance for NH_4^+-N removal, whereby ammonia-nitrogen can be adsorbed by the media during the rainy season and then removed through nitrification in the dry season (Cho et al., 2009).

3.2. Surface characteristics of RHB and ICB

The surface structures of the RHB and ICB shown in Fig. 2 demonstrates the presence of some particulate matter on the surface of ICB, which may be attached ferric ions. In addition, the surface of ICB is more plumped than RHB, which explains the bigger surface area measured for the ICB than RHB.

The FTIR spectra (wavenumbers 4000-500 cm^{-1}) shown in Fig. 3 indicate distinct absorption peaks at the same place for both RHB and ICB mainly at 3723, 3437, 1637, 1562, 1426, 1069, 873 and 778. The occurrence of similar characteristic absorption peaks for the two materials indicates that the surfaces of both biochar materials contain roughly the same surface functional groups. The broad peaks at 3500-3200 cm^{-1} indicate the stretching and vibration of hydroxy(-OH). Nonetheless, the absorption peak of ICB is wider, indicating more abundant hydroxyl functional groups on the ICB. Conversely, the peaks at 1000-1500 cm^{-1} indicate the stretching vibration of a single bond containing no hydrogen. Overall, ICB demonstrates a wider absorption peak and a higher strength.

3.3. Adsorption of NH_4^+-N by RHB and ICB

Figure S1 illustrates the adsorption isotherms for NH_4^+-N by RHB and ICB. In Fig. S1, q_e is the amount adsorbed (mg/g), and C_e is the equilibrium solution concentrations (mg/L). The results of the Langmuir model fitting (Table S1) showed that both RHB and ICB had good adsorption capacities for NH_4^+-N. The maximum adsorption capacity of ICB for NH_4^+-N is higher than that of RHB, which is consistent with its specific surface area and CEC. The parameter R_L for both RHB and ICB ranged between 0 and 1, indicating that the adsorption of NH_4^+-N by either RHB or ICB will proceed with ease.

3.4. Removal of COD in different experimental columns

The removal of COD in the various experimental columns shown in Fig. 4(a) indicates an average removal rate of less than 80% in the $5^{\#}$ experimental column, which is lower than that of the other experimental columns. The $1^{\#}$ experimental column showed better performance than the $2^{\#}$ experimental column for COD removal. Similarly, the $3^{\#}$ experimental column showed better performance

Table 1
Physicochemical properties of ICB, RHB, SOIL, SAND.

Property	ICB	RHB	SOIL	SAND
pH [a]	2.905 ± 0.075	8.275 ± 0.455	7.345 ± 0.065	8.230 ± 0.160
Ash [a]/%	38.52 ± 0.57	42.2 ± 80.69	89.20 ± 0.03	96.72 ± 0.7
CEC [a]/(mmol/kg)	81.251 ± 0.3	67.743 ± 0.5	7.000 ± 0.1	1.5000 ± .4
ζ-potential [a]/mV	−5±0.05	−3±0.03	−1.37 ± 0.03	−16 ± 0.02
Specific surface [a]/(m^2/g)	170 ± 3	150 ± 5	—	11.8 ± 0.6

— Didn't measure.
[a] Average ± standard deviation.

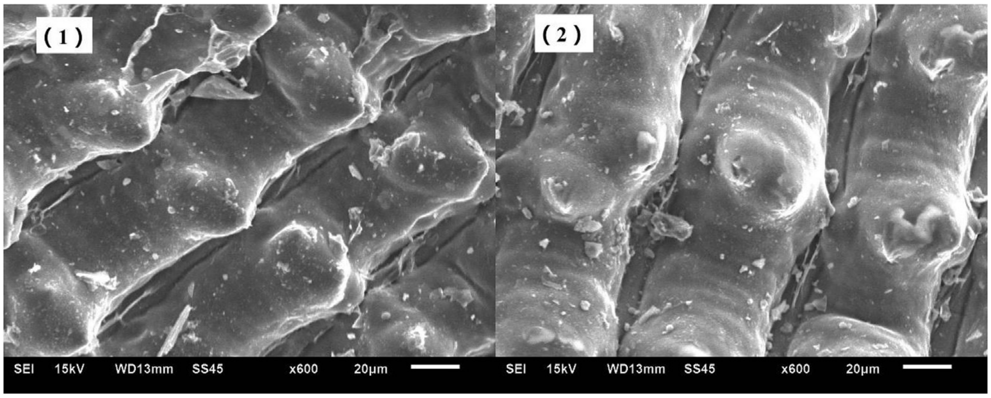

Fig. 2. SEM images of RHB (1) and ICB (2).

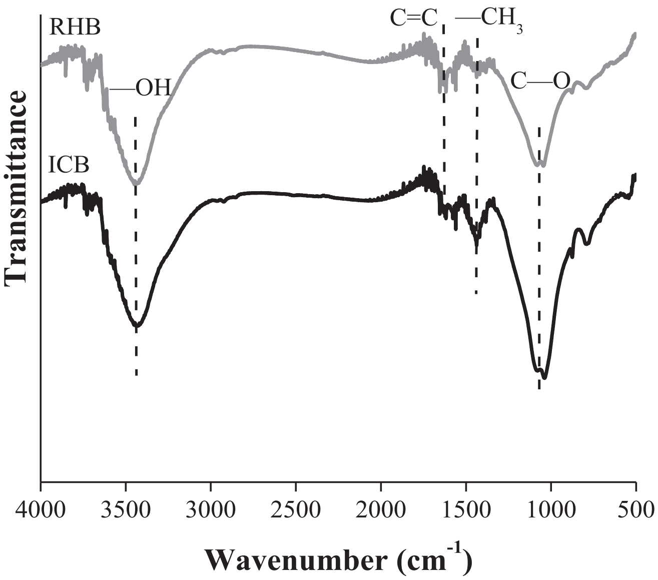

Fig. 3. FTIR spectra of RHB and ICB.

than the $4^{\#}$ experimental column for COD removal. The average COD removal rates for $1^{\#}$ and $3^{\#}$ experimental columns were over than 90%, whereas those for the $2^{\#}$ and $4^{\#}$ experimental columns ranged between 80 and 90%. This finding shows that each biochar type improves the media to create an environment suitable for microbial growth, and ICB is particularly suitable for microbial growth and beneficial for the removal of organic matter. Reports from previous studies (Chen et al., 2013) demonstrate that the amounts of bacteria 16 sDNA in the media is positively correlated with organic matter, which also provides theoretical support for the biochar-amended bioretention cells. In addition, the removal performance of the $1^{\#}$ and $3^{\#}$ experimental columns were similar, whereas those of the $2^{\#}$ and $4^{\#}$ experimental columns were similar. These findings also indicate that the removal of COD in the experimental column mainly occurred in the upper layers of the media.

3.5. *Removal of N in different experimental columns*

The removal of NH_4^+-N in the various experimental columns is shown in Fig. 4(b). By comparison, the removal of NH_4^+-N was worst in the $5^{\#}$ experimental column, with removal rates ranging between 85 and 90%. The $3^{\#}$ experimental column showed the best overall performance, with a relatively stable average NH_4^+-N removal efficiency of over 95%, and an upper limit of up to 98%. In addition, the $1^{\#}$ experimental column also showed a stable NH_4^+-N removal, but the average removal rate was less than that of the $3^{\#}$ experimental column. Nevertheless, the removal efficiencies of the $2^{\#}$ and $4^{\#}$ experimental columns exhibited a downward trend after the 9th day of the experimental operation and finally fell below the level of the $1^{\#}$ experimental column on the 11th day. This finding indicates that the adsorption capacity of the ICB-amended media for NH_4^+-N is higher than that of the RHB-amended media. Moreover, the stability of the effluent quality in the RHB-amended media was poorer. Overall, the NH_4^+-N removal performance in the $3^{\#}$ experimental column is similar to that of the $1^{\#}$ experimental column, whereas that of the $4^{\#}$ experimental column is similar to that of the $2^{\#}$ experimental column. These results demonstrate that the removal of NH_4^+-N in the experimental columns mainly occurs in the upper part of the media. It may be that the NH_4^+-N adsorbed by the media is finally converted to NO_3^--N through nitrification, which has been shown in some previous studies (Cho et al., 2009).

The removal of NO_3^--N in the various experimental columns shown in Fig. 4(c) demonstrates superior NO_3^--N removal effects in both $3^{\#}$ and $4^{\#}$ experimental columns. The $4^{\#}$ experimental column, where the NO_3^--N removal rate exceeded 90%, was the most stable and efficient. The $3^{\#}$ experimental column was second to the $4^{\#}$ experimental column for NO_3^--N removal, with an average removal efficiency of over 80%. The removal efficiencies of the $1^{\#}$ and $2^{\#}$ experimental columns for NO_3^--N exceeded 55% at the beginning of the experiment. However, as the experiment proceeded, the removal efficiency gradually declined to about 20%, which is considerably lower than that achieved in the $5^{\#}$ experimental column. The results of the $1^{\#}$ and $2^{\#}$ experimental columns may be attributed to the trapping of nitrate in the water in the upper part of the media, and the fact that the NH_4^+-N adsorbed onto the media is not readily converted into NO_3^--N by nitrification. Consequently, the removal of NO_3^--N remains relatively high, but as the experiment proceeds, the NO_3^--N in the upper parts of the media enters the lower part, and the NH_4^+-N adsorbed on the media is further converted to nitrate. However, because there is not enough carbon available in the lower parts of the $1^{\#}$ and $2^{\#}$ experimental columns, denitrification reaction is weak, resulting in NO_3^--N leaching. Contrary to this, the addition of biochar in the lower parts of the $3^{\#}$ and $4^{\#}$ experimental columns provides sufficient carbon sources for denitrification reactions and, also, provides a suitable living environment for microbial attachment and growth (Sun et al., 2018). For the removal of NO_3^--N, soil microbes play an important role compared to soil adsorption and chemical precipitation (Xu et al., 2014). With the growth of microorganisms, denitrification in the soil is significantly enhanced. Consequently,

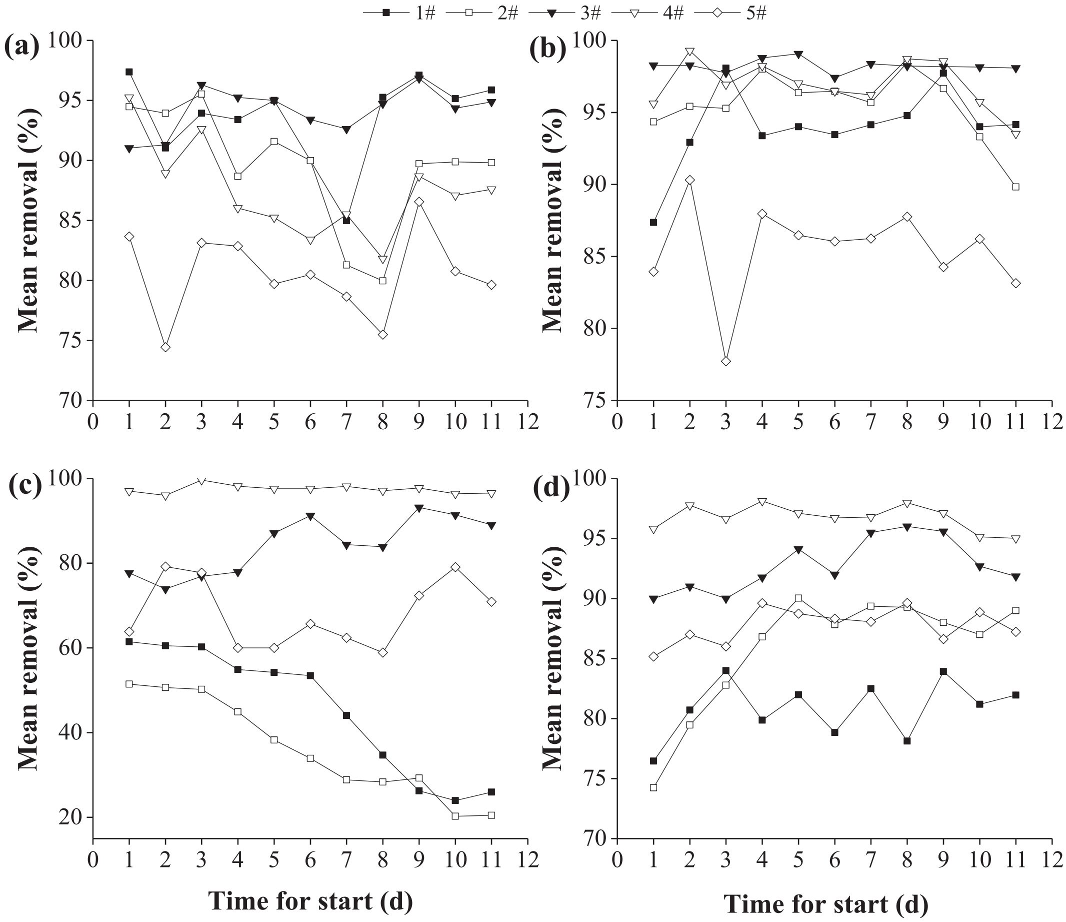

Fig. 4. Removal effect of COD and N through bioretention. (a) COD, (b)NH_4^+-N, (c)NO_3^--N and (d)TN.

the removal of NO_3^--N is attributed to the assimilation and dissimilation of microorganisms using NO_3^--N. This result was also validated in Fig. 5(a), which shows that the DEA at the bottom of the media in the $3^\#$ and $4^\#$ experimental columns were significantly higher than that those in the $1^\#$ and $2^\#$ experimental columns. This finding is consistent with that illustrated in Fig. 4(c) and is also consistent with the results of other researchers (Zhang et al., 2011). However, at the media boundary layer (height 550 mm), the result is just the opposite. This disparity may be due to the difference in constituents of the upper and lower layers of the media. The upper layer media of both $1^\#$ and $2^\#$ experimental columns contain biochar, whereas the lower layer media has none. This structure causes

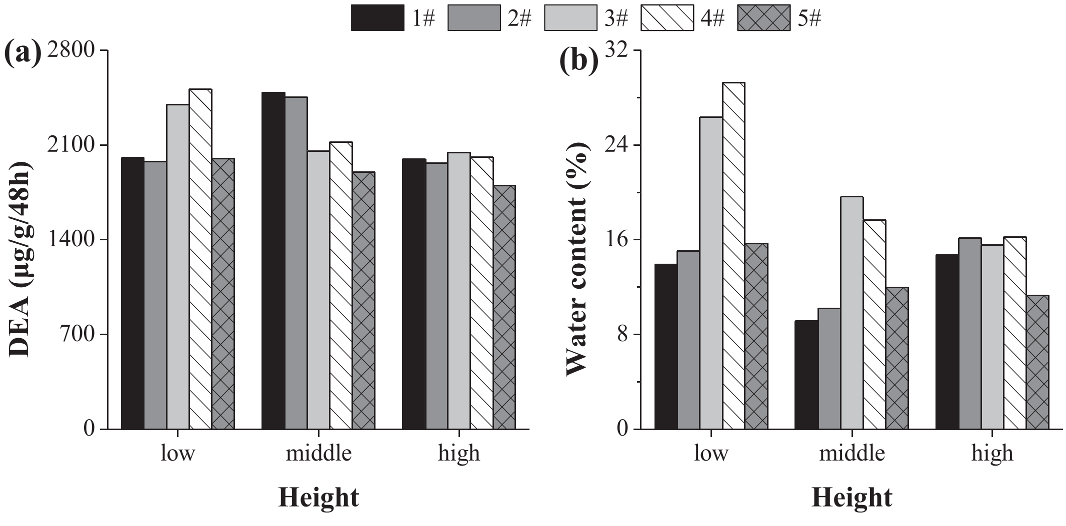

Fig. 5. Denitrifying enzyme activity(a) and water content(b) of media for different heights.

the permeability coefficient of the upper layer of the experimental column to be larger than that of the lower layer. Nonetheless, part of the biochar in the upper layer can enter into the upper part of the lower layer of the media, resulting in a mixed layered interfacial filler. This unique structure may create an environment that promotes the denitrification process. There are also studies suggesting that the number of denitrifying bacteria increases within the transition from aerobic to anaerobic conditions (Ma et al., 2017). The presence of biochar at the boundary also provides a more diversified cell-soil boundary for microbial species abundance and protein expression (Hanzel et al., 2013). These factors explain the higher DEA in the boundary layer. At the same time, Fig. 5(b) indicates that the water content at the bottom of the media in the 3$^{\#}$ and 4$^{\#}$ experimental columns were notably higher than those in the other experimental columns. The reason for this result is that biochar amendment significantly increased soil water retention, which is attributed to the large pore volume of biochar (Tian et al., 2019). As such, biochar amendment in the saturated zone would promote redox conditions conducive to denitrification. So, this finding is consistent with that illustrated in Fig. 4(c).

The TN removal efficiency of the various experimental columns shown in Fig. 4(d) indicates significantly higher performance of the 4$^{\#}$ experimental column than those of the 3$^{\#}$ and 5$^{\#}$ experimental columns, which stabilizes at an average of 95%. Similarly, the TN removal performance of 3$^{\#}$ and 4$^{\#}$ experimental columns are significantly higher than those of 1$^{\#}$ and 2$^{\#}$ experimental columns.

Overall, the experimental columns perform roughly the same for the removal of nitrate. It has also been demonstrated that the limiting factor to the removal of N in the experimental columns is the removal of nitrate. In general, the use of amended media in the experimental column offer better opportunities for improved N removal.

3.6. *Removal of phosphorus in different experimental columns*

The columns showed significant differences in the removal of TP. As shown in Fig. 6(a), the removal rates of the 2$^{\#}$ and 4$^{\#}$ experimental columns are lower, whereas those of the 1$^{\#}$, 3$^{\#}$, and 5$^{\#}$ experimental columns is better. This finding is consistent with the experimental results reported by Li et al. (2014), which proves that the ICB-amended media significantly reduces the leaching of available phosphorus. The poor TP removal efficiencies of the 2$^{\#}$ and 4$^{\#}$ experimental columns may be due to the phosphorus leaching from the biochar itself, or it may be due to the setting of the saturated zone. On the one hand, the anaerobic conditions generated by the setting of the saturated zone may induce leaching of dissolved phosphorus and, subsequently, the increase of TP, which may be caused by iron-reducing bacteria (Baldwin and Mitchell, 2000). On the other hand, the low-oxygen conditions induced by the setting of the saturated zone are likely to cause a mobilization and export of previously particle-bound P from the filter material (Correll, 1999). This release of soil-bound phosphorus from the filter material under anaerobic conditions has been studied (Clausen and Dietz, 2006). The 1$^{\#}$ and 3$^{\#}$ experimental columns comprise of ICB, which causes the P and filler to form stronger bonds (Bohn et al., 2001).

Fig. 6(b) shows TP concentrations in media samples from different depths of each experimental column at the end of the simulated runoff experiment. It can be seen that the amount of phosphorus intercepted in each experimental column decreases with depth. In the middle and upper zones, the 1$^{\#}$ and 3$^{\#}$ experimental columns showed higher interception rates of phosphorus than that of the other experimental columns. The interception rate of phosphorus in the 2$^{\#}$ and 4$^{\#}$ experimental columns in the upper zone is higher than that of the 5$^{\#}$ experimental column but less than the 5$^{\#}$ experimental column in the middle and lower zones. These results further illustrate the findings observed in Fig. 6(a). Also, the results show that a certain minimum packing depth is required for the efficient removal of phosphorus. Similar findings have also been reported in other studies (Davis et al., 2006).

4. Conclusions

The effects of incorporating rice husk biochar (RHB) or iron-coated biochar (ICB) into the media of bioretention systems were tested using column trials. The results demonstrate that for the removal of COD, NH$_4^+$-N, and TP, the performance of ICB-amended columns was the best. The findings also indicate that the removal of NH$_4^+$-N in the experimental columns mainly occurs in the upper part of the media. Media amended with either RHB or ICB showed average NH$_4^+$-N removal rates higher by 9%–17% than that of the conventional media. For the removal of NO$_3^-$-N and TN, the columns with only a single layer and amended with either RHB or ICB exhibited the best performance. This finding proved that adding biochar into the saturated zone can facilitate denitrification to enhance NO$_3^-$-N removal significantly. Also, incorporating ICB into

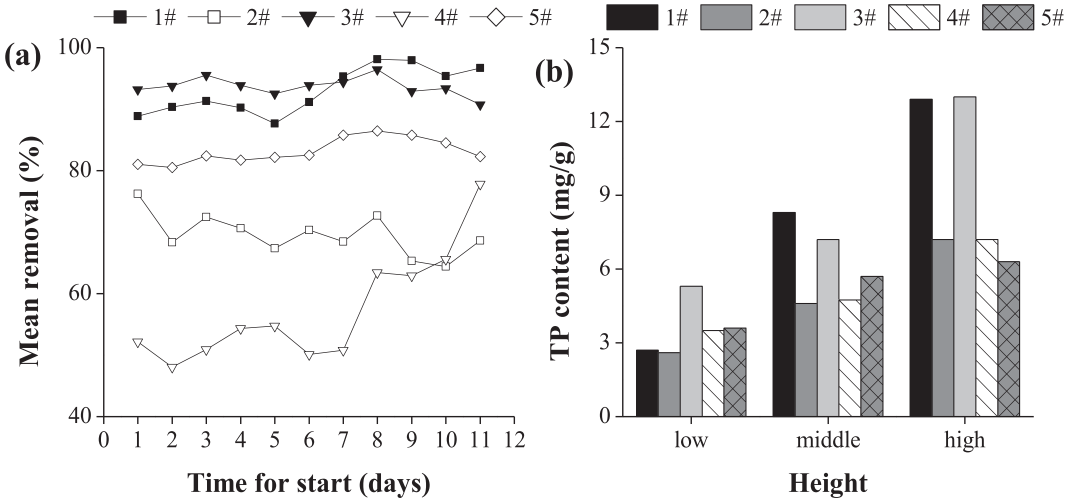

Fig. 6. Removal effect of TP through bioretention(a) and removal of TP by different experimental columns on different heights of media(b).

the upper layers of bioretention cells media can effectively enhance the TP removal performance. Nonetheless, the TP removal diminished with the addition of RHB into the media.

Overall, the results of this study demonstrate that the addition of either RHB or ICB into the media of bioretention cells is recommended if N discharges pose a potential threat to the receiving environment. However, if P concentrations are of principal concern, adding RHB would be counterproductive.

Acknowledgements

This work is supported by the National Program of Water Pollution Control (Grant No. 2012ZX07308-001-08), the Program for Changjiang Scholars and Innovative Research Team in University (Grant No. IRT0853), the Shaanxi Innovative Research Team Program for Key Science and Technology, the Key Research and Development Program of Shaanxi Province (Grant No. 2018KWZ-11), the National Natural Science Foundation of China (Grant No. 51808442), and the Natural Science Basic Research Plan of Shaanxi Province (Grant No. 2019JQ-529).

Appendix A. Supplementary data

Supplementary data to this article can be found online at https://doi.org/10.1016/j.chemosphere.2019.124424.

References

Baldwin, D.S., Mitchell, A.M., 2000. The effects of drying and re-flooding on the sediment and soil nutrient dynamics of lowland river—floodplain systems: a synthesis. Regul. Rivers Res. Manag. 16, 457—467.

Bohn, H.L., McNeal, B.L., O'Connor, G.A., 2001. Soil Chemistry, third ed. John Wiley & Sons, Ins., New York, USA.

Bratieres, K., Fletcher, T.D., Deletic, A., Zinger, Y., 2008. Nutrient and sediment removal by stormwater biofilters: a large-scale design optimisation study. Water Res. 42, 3930—3940.

Chen, X.L., Peltier, E., Sturm, B.S.M., Young, C.B., 2013. Nitrogen removal and nitrifying and denitrifying bacteria quantification in a stormwater bioretention system. Water Res. 47, 1691—1700.

Cho, K.W., Song, K.G., Cho, J.W., Kim, T.G., Ahn, K.H., 2009. Removal of nitrogen by a layered soil infiltration system during intermittent storm events. Chemosphere 76, 690—696.

Clausen, J.C., Dietz, M.E., 2006. Saturation to improve pollutant retention in a rain garden. Environ. Sci. Technol. 40, 1335—1340.

Correll, D.L., 1999. Phosphorus: a rate limiting nutrient in surface waters. Poult. Sci. 78, 674—682.

Davis, A.P., Shokouhian, M., Sharma, H., Minami, C., 2001. Laboratory study of biological retention for urban stormwater management. Water Environ. Res. 73, 5—14.

Davis, A.P., Shokouhian, M., Sharma, H., Minami, C., 2006. Water quality improvement through bioretention media: nitrogen and phosphorus removal. Water Environ. Res. 78, 284—293.

Davis, A.P., Hunt, W.F., Traver, R.G., Clar, M., 2009. Bioretention technology: overview of current practice and future needs. J. Environ. Eng. 135 (3), 109—117.

Hanzel, J., Myrold, D., Sessitsch, A., Smalla, K., Tebbe, C.C., Totsche, K.U., 2013. Microbial ecology of biogeochemical interfaces - diversity, structure, and function of microhabitats in soil. FEMS Microbiol. Ecol. 86, 1—2.

Hatt, B.E., Fletcher, T.D., Deletic, A., 2009. Hydrologic and pollutant removal performance of stormwater biofiltration systems at the field scale. J. Hydrol. 365, 310—321.

Hsieh, C.-h., Davis, A.P., Needelman, B.A., 2007. Nitrogen removal from urban stormwater runoff through layered bioretention columns. Water Environ. Res. 79 (12), 2404—2411.

Hunt, W.F., Jarrett, A.R., Smith, J.T., Sharkey, L.J., 2006. Evaluating bioretention hydrology and nutrient removal at three field sites in North Carolina. J. Irrig. Drain. Eng. 132, 600—608.

Hunt, W.F., Davis, A.P., Traver, R.G., 2012. Meeting hydrologic and water quality goals through targeted bioretention design. J. Environ. Eng. 138 (6), 698—707.

Jiang, C.B., Li, J.K., Li, H.E., Li, Y.J., Chen, L., 2017. Field performance of bioretention systems for runoff quantity regulation and pollutant removal. Water Air Soil Pollut. 228 (12), 468.

Jing, T., 2016. The Effect of Biochar on Bioretention Hydrologic Effect and Nitrogen Removal. Southwest Jiaotong University, Chengdu, China, p. 129.

Kim, M.H., Sung, C.Y., Li, M.H., Chu, K.H., 2012. Bioretention for stormwater quality improvement in Texas: removal effectiveness of escherichia coli. Separ. Purif. Technol. 84, 120—124.

Li, H., Davis, A.P., 2009. Water quality improvement through reductions of pollutant loads using bioretention. J. Environ. Eng. 135, 567—576.

Li, L., Davis, A.P., 2014. Urban stormwater runoff nitrogen composition and fate in bioretention systems. Environ. Sci. Technol. 48, 3403—3410.

Li, J.H., Lv, G.H., Bai, W.B., Liu, Q., Zhang, Y.C., Song, J.Q., 2014. Modification and use of biochar from wheat straw (triticum aestivum l.) for nitrate and phosphate removal from water. Desalin. Water Treat., pp. 1—13

Liu, J.Y., Davis, A.P., 2014. Phosphorus speciation and treatment using enhanced phosphorus removal bioretention. Environ. Sci. Technol. 48, 607—614.

Lopez-Ponnada, E.V., Lynn, T.J., Peterson, M., Ergas, S.J., Mihelcic, J.R., 2017. Application of denitrifying wood chip bioreactors for management of residential non-point sources of nitrogen. J. Biol. Eng. 11 (1).

Ma, W.W., Han, Y.X., Ma, W.C., Han, H.J., Zhu, H., Xu, C.Y., Li, K., Wang, D.X., 2017. Enhanced nitrogen removal from coal gasification wastewater by simultaneous nitrification and denitrification (SND) in an oxygen-limited aeration sequencing batch biofilm reactor. Bioresour. Technol. 244, 84—91.

Macedo, M.B.d., Lago, C.A.F.d., Mendiondo, E.M., 2019. Stormwater volume reduction and water quality improvement by bioretention: potentials and challenges for water security in a subtropical catchment. Sci. Total Environ. 647, 923—931.

Ministry of Ecology and Environment of the Prople's Republic of China (MOEE), 2013. Soil — Determination of Exchangeable Acidity by Potassium Chloride Extraction —titration Method. China Environment Publishing Group, Beijing, China.

Ministry of Ecology and Environment of the Prople's Republic of China (MOEE), 2014. Soil Quality—Determination of Available Phosphorus—Sodium Hydrogen Carbonate Solution-Mo-Sb Anti Spectrophotometric Method. China Environment Publishing Group, Beijing, China.

Mohanty, S.K., Valenca, R., Berger, A.W., Yu, I.K.M., Xiong, X.N., Saunders, T.M., Tsang, D.C.W., 2018. Plenty of room for carbon on the ground: potential applications of biochar for stormwater treatment. Sci. Total Environ. 625, 1644—1658.

Ministry of Housing and Urban-Rural Development of the People's Republic of China (MOHURD), 2014. Sponge City Construction Technical Guide——low impact development of rainwater system construction. China Architecture & Building press, Beijing, China.

NCDWQ, 2007. Bioretention. Stormwater best management practices manual. N.C. Department of Environmental and Natural Resources, Divison of Water Quality, Raleigh, pp. 12—13.

Nielsen, T.H., Revsbech, N.P., 1998. Nitrification, denitrification, and n-liberation associated with two types of organic hotsports in soil. Soil Biol. Biochem. 30, 611—619.

Richardson, J.L., Vepraskas, M.J., 2015. Wetland soils—genesis, hydrology, landscapes, and classification, second ed. CRC Press LLC, Boca Raton, Florida.

Sun, X., Davis, A.P., 2007. Heavy metal fates in laboratory bioretention systems. Chemosphere 66, 1601—1609.

Sun, J.J., Chen, L., Rene, E.R., Hu, Q., Ma, W.F., Shen, Z.Y., 2018. Biological nitrogen removal using soil columns for the reuse of reclaimed water: performance and microbial community analysis. J. Environ. Manag. 217, 100—109.

Tan, K.H., 2005a. Cation exchange capacity and % base saturation determination. In: Tan, K.H. (Ed.), Soil Sampling, Preparation, and Analysis. CRC Press LLC, Boca Raton, pp. 215—239.

Tan, K.H., 2005b. Sample preparation. In: Tan, K.H. (Ed.), Soil Sampling, Preparation, and Analysis. CRC Press LLC, Boca Raton, pp. 29—41.

Tian, J., Miller, V., Chiu, P.C., Maresca, J.A., Guo, M.X., Imhoff, P.T., 2016. Nutrient release and ammonium sorption by poultry litter and wood biochars in stormwater treatment. Sci. Total Environ. 553, 596—606.

Tian, J., Jin, J., Chiu, P.C., Cha, D.K., Guo, M.X., Imhoff, P.T., 2019. A pilot-scale, bi-layer bioretention system with biochar and zero-valent iron for enhanced nitrate removal from stormwater. Water Res. 148, 378—387.

Trowsdale, S.A., Simcock, R., 2011. Urban stormwater treatment using bioretention. J. Hydrol. 397, 167—174.

Wan, Z.X., Li, T., Shi, Z.B., 2017. A layered bioretention system for inhibiting nitrate and organic matters leaching. Ecol. Eng. 107, 233—238.

Xu, H.-J., Wang, X.-H., Li, H., Yao, H.-Y., Su, J.-Q., Zhu, Y.-G., 2014. Biochar impacts soil microbial community composition and nitrogen cycling in an acidic soil planted with rape. Environ. Sci. Technol. 48, 9391—9399.

Xu, N., Tan, G.C., Wang, H.Y., Gai, X.P., 2016. Effect of biochar additions to soil on nitrogen leaching, microbial biomass and bacterial community structure. Eur. J. Soil Biol. 74, 1—8.

Zhang, Z.H., Rengel, Z., Liaghati, T., Antoniette, T., Meney, K., 2011. Influence of plant species and submerged zone with carbon addition on nutrient removal in stormwater biofilter. Ecol. Eng. 37, 1833—1841.

Zinger, Y., Blecken, G.T., Fletcher, T.D., Viklander, M., Deletic, A., 2013. Optimising nitrogen removal in existing stormwater biofilters: benefits and tradeoffs of a retrofitted saturated zone. Ecol. Eng. 51, 75—82.